Published in final edited form as:
Dev Cell. 2010 January 19; 18(1): 25. doi:10.1016/j.devcel.2009.11.014.

Local Protease Signaling Contributes to Neural Tube Closure in the Mouse Embryo

Eric Camerer[1,2,4], **Adrian Barker**[1], **Daniel N. Duong**[1], **Rajkumar Ganesan**[5], **Hiroshi Kataoka**[1,*], **Ivo Cornelissen**[1], **Molly R. Darragh**[3], **Arif Hussain**[1], **Yao-Wu Zheng**[1], **Yoga Srinivasan**[1], **Christopher Brown**[3], **Shan-Mei Xu**[1], **Jean B. Regard**[1,**], **Chen-Yong Lin**[6], **Charles S. Craik**[3], **Daniel Kirchhofer**[5], and **Shaun R. Coughlin**[1,2]

[1] Cardiovascular Research Institute, University of California, San Francisco, CA 94158, USA

[2] Department of Medicine, University of California, San Francisco, CA 94158, USA

[3] Department of Biochemistry, University of California, San Francisco, CA 94158, USA

[4] INSERM Unit 970, Equipe Avenir, Paris Cardiovascular Research Center, 75737 Paris Cedex 15, France

[5] Department of Protein Engineering, Genentech Inc., South San Francisco, CA 94080, USA

[6] Department of Biochemistry and Molecular Biology, University of Maryland, Baltimore, MD 21201, USA

Summary

We report an unexpected role for protease signaling in neural tube closure and formation of the central nervous system. Mouse embryos lacking protease-activated receptor 1 and 2 showed defective hindbrain and posterior neuropore closure and developed exencephaly and spina bifida, important human congenital anomalies. *Par1* and *Par2* were expressed in surface ectoderm, *Par2* selectively along the line of closure. Ablation of $G_{i/z}$ and Rac1 function in these *Par2*-expressing cells disrupted neural tube closure, further implicating G protein-coupled receptors and identifying a likely effector pathway. Cluster analysis of protease and Par2 expression patterns revealed a group of membrane-tethered proteases often co-expressed with Par2. Among these, matriptase activated Par2 with picomolar potency, and hepsin and prostasin activated matriptase. Together, our results suggest a role for protease-activated receptor signaling in neural tube closure and identify a local protease network that may trigger Par2 signaling and monitor and regulate epithelial integrity in this context.

Introduction

Protease-activated receptors (PARs) are G protein-coupled receptors (GPCRs) that allow cells to sense specific proteases in their environment (Coughlin, 2000; Vu et al., 1991). Four PARs are found in humans and mice. PARs 1, 3, and 4 mediate cellular responses to the coagulation protease thrombin. PAR2 is not activated effectively by thrombin but can be activated by a

Corresponding author: S. Coughlin, University of California, San Francisco, 600 16th Street, San Francisco, CA 94158-2240, USA. Phone: (415) 476 6174 Fax: (415) 476 8173 shaun.coughlin@ucsf.edu.
*Present address: Riken Center for Developmental Biology, Kobe, Japan
**Present address: National Institutes of Health, Bethesda, MD 20892-4472, USA

variety of serine proteases with trypsin-like specificity including the coagulation proteases tissue factor/factor VIIa and factor Xa (Camerer et al., 2000; Riewald and Ruf, 2001). Studies in cell culture, animal models and humans support the view that, in the adult, PARs and the coagulation cascade couple tissue injury with vascular damage to appropriate cellular responses that regulate hemostasis, inflammation, cell survival and tissue repair (Becker et al., 2009; Camerer et al., 2004; Coughlin, 2000; Coughlin and Camerer, 2003; Guo et al., 2004; Kahn et al., 1999; Sambrano et al., 2001; Vergnolle et al., 2001).

Less is known regarding the roles of PARs and the proteases that activate them in contexts other than tissue injury, particularly in embryonic development. Par1-deficient mouse embryos exhibit partially penetrant lethality at midgestation due to lack of Par1 signaling in endothelial cells (Connolly et al., 1996; Griffin et al., 2001). This phenotype is less penetrant and less severe than that associated with knockout of tissue factor, the trigger for coagulation (Mackman, 2004). Toward testing the possibility that this difference might be due to partially redundant functions of Par1 and other PARs downstream of tissue factor and the coagulation cascade, we generated mice lacking multiple PARs and uncovered an unexpected phenotype associated with combined knockout of the genes encoding Par1 and Par2: failed neural tube closure. We also characterized a set of membrane-tethered proteases that may comprise a local protease network that activates Par2 during neural tube closure, and we identified G_i and Rac as candidate downstream effectors of Par2 and other GPCRs in this process. This system appears to operate in the surface ectoderm along the line of closure. Together, our studies identify an unexpected role for local protease/PAR signaling in neural tube closure, a process that is critical for formation of the central nervous system and that goes awry in the congenital anomalies exencephaly and spina bifida.

Results

Combined deficiency in *Par1* and *Par2* results in defective neural tube closure

Par1 and *Par2* are just 76kb apart on mouse chromosome 13 (see Experimental Procedures for gene nomenclature). Given this linkage, we generated the *Par1:Par2* double knockout by using homologous recombination to disrupt the *Par1* gene in mouse embryonic stem (ES) cells in which the *Par2* gene had been previously targeted (Camerer et al., 2002). Each recombination inserted a β-galactosidase (lacZ) coding sequence at the start codon so as to substitute lacZ for Par1 and Par2 expression (Griffin et al., 2001) (Figure S1A). Crosses of $Par1^{+/-}$:$Par2^{+/-}$ mice generated from ES cells in which *Par1* and *Par2* were disrupted on the same chromosome produced live $Par1^{-/-}$:$Par2^{-/-}$ offspring at weaning at 4.6–7.6% of the expected Mendelian rate in a mixed 129/BL6 background (Figure S1B). In the same genetic background, $Par1^{+/-}$ crosses produced $Par1^{-/-}$ offspring at ~50% of the expected rate and $Par2^{+/-}$ crosses produced $Par2^{-/-}$ offspring at ~85% of the expected rate ((Connolly et al., 1996; Damiano et al., 1999; Griffin et al., 2001) and not shown). Thus, combined deficiency of Par1 and Par2 produced much more penetrant embryonic lethality than isolated Par1 or Par2 deficiency. $Par1^{-/-}$:$Par2^{-/-}$ embryos showed three different phenotypes, each partially penetrant: midgestational cardiovascular failure beginning at 9.5 dpc as previously described with isolated Par1 deficiency (Connolly et al., 1996; Griffin et al., 2001), exencephaly, and late gestational lethality associated with widespread edema (Figure 1A). In the same strain background, exencephaly was not observed in either single knockout and late gestational lethality was seen only infrequently in $Par2^{-/-}$ embryos. Thus, these two phenotypes appear to reflect interacting roles of Par1 and Par2 in the developing embryo. Occasional $Par1^{-/-}$:$Par2^{-/-}$ mice did survive embryonic development, and these sometimes exhibited spina bifida and curly tail (Figure 1A). Exencephaly, spina bifida, and curly tail are all hallmarks of failed neural tube closure (Copp et al., 2003). Thus, $Par1^{-/-}$:$Par2^{-/-}$ mice appeared to have an incompletely penetrant defect in closure of both hindbrain and posterior

neuropores. Because no role for PARs in the development of the nervous system has been described, we focused on characterizing this phenotype.

Exencephaly was detectable by gross inspection beginning at 11.5 dpc; 17/51 (33%) viable *Par1*$^{-/-}$*:Par2*$^{-/-}$ embryos exhibited exencephaly after that time (Figure 1A,B). Restoring Par1 expression in endothelial cells with a Tie2p/e-Par1 transgene (Griffin et al., 2001) rescued the midgestational lethality in *Par1*$^{-/-}$*:Par2*$^{-/-}$ embryos but did not prevent exencephaly (Figure 1C), implying that neither loss of Par1 function in endothelial cells nor midgestational cardiovascular failure contributed to the exencephaly phenotype.

Exencephaly is due to defective closure of the hindbrain neuropore. To directly assess neuropore closure, we scored embryos from *Par1*$^{-/-}$*:Par2*$^{-/-}$ X *Par1*$^{+/-}$*:Par2*$^{+/-}$ crosses for an open or closed hindbrain neuropore and somite count before genotyping. 22% of *Par1*$^{+/-}$*:Par2*$^{+/-}$ embryos collected at 9.5 dpc had open hindbrain neuropores compared to 47% of *Par1*$^{-/-}$*:Par2*$^{-/-}$ embryos (Figure 1D). Among embryos that had progressed to the 15-somite stage or beyond, only 4% of controls had open neuropores vs. 32% of mutants (Figure 1D,E). The latter frequency is similar to the overall penetrance of exencephaly in the mutants. These results suggest that exencephaly in *Par1*$^{-/-}$:*Par2*$^{-/-}$ embryos is a result of failed closure of the hindbrain neuropore and that such failure is not simply a result of developmental delay.

Par2 is expressed in the surface ectoderm adjacent to the neuroepithelium at the time and place of neural tube closure

A direct role for PARs in neural tube closure would demand expression of the receptors in or around the neural tube at the time of closure. β-galactosidase staining of *Par2-LacZ* knockin embryos revealed expression of *Par2* in the surface ectoderm cells immediately overlying the neuroepithelium at the time and place of fusion (Figure 2A,B and Figure S2A,B). Such localized *Par2* expression was confirmed by in situ hybridization of wild-type embryos for *Par2* mRNA (Figure 2C and Figure S2C). By the same measures, *Par1* expression was detected in endocardium, endothelium and a subset of hematopoietic cells but not in surface ectoderm (Figure S2D). However, *Par1* mRNA was readily detected by quantitative PCR of RNA from FACS-sorted surface ectoderm cells (see below) suggesting that Par1 is probably expressed in surface ectoderm at levels below the detection limits of the other techniques. Thus, while we cannot exclude less direct mechanisms, the requirement for knockout of both *Par1* and *Par2* for the appearance of exencephaly may be due to partially redundant functions of these receptors in the surface ectoderm.

Together with the exencephaly phenotype in *Par1*$^{-/-}$:*Par2*$^{-/-}$ embryos, the precise expression of Par2 at the place and time of neural tube closure suggested an unexpected role for local Par2 signaling in surface ectoderm in neural tube closure. These observations prompted an effort to obtain independent evidence for the importance of GPCR signaling in surface ectoderm during neural tube closure.

Surface ectoderm-specific knockout of G_i and Rac1 function, signaling pathways downstream of Par2, causes neural tube defects

If loss of GPCR function in surface ectoderm is responsible for the neural tube closure defects described above, surface ectoderm-specific knockout of the relevant signaling pathway(s) downstream of GPCRs should also cause neural tube defects. To manipulate genes in surface ectoderm, we generated mice in which a Cre-IRES-NLSlacZ cassette was inserted in the Grainyhead-like-3 (*Grhl3*) gene (Figure S3A), hereafter designated *Grhl3*$^{Cre/+}$ mice. Grhl3 is a transcription factor expressed in surface ectoderm, hindgut endoderm and other epithelial cells in a pattern similar to Par2 at the time of neural tube closure (Figure 2), and loss of Grhl3 function causes exencephaly and spina bifida in knockout and curly tail (*ct/ct*) mutant mice

((Auden et al., 2006; Gustavsson et al., 2007; Ting et al., 2003); Figure 2A-D and Figure S3)). X-gal staining of *Grhl3*$^{Cre/+}$ embryos collected at 8.5 dpc confirmed NLSlacZ expression in surface ectoderm along the neural ridge in a pattern that was indistinguishable from *Par2* (Figure 2); expression quickly spread laterally from the neural ridge to cover much of the surface ectoderm. In accord, examination of *Grhl3*$^{Cre/+}$ embryos carrying a cytoplasmic lacZ or YFP Cre-excision reporter revealed reporter expression first in the midline then spreading laterally in the surface ectoderm to cover the embryo (Figure S3B-D). Thus, the *Grhl3*^{Cre} allele drove efficient and relatively tissue-specific excision of floxed sequences in surface ectoderm. *Grhl3*$^{Cre/Cre}$ embryos — effectively *Grhl3* nulls — recapitulated the neural tube defect phenotypes reported for *Grhl3*$^{-/-}$ embryos (Ting et al., 2003), but, importantly, *Grhl3*$^{Cre/+}$ embryos (effectively *Grhl3* heterozygotes) had no neural tube phenotype in the absence of a relevant floxed target allele.

Par1 and Par2 can couple to members of the $G_{q/11}$, $G_{i/o/z}$, and $G_{12/13}$, G protein subfamilies (Coughlin, 2000), although Par2 coupling to $G_{12/13}$ may be less effective than Par1 (Vouret-Craviari et al., 2003). Combined deficiency in $G\alpha_q$ and $G\alpha_{11}$ causes embryonic lethality around 11 dpc; neural tube defects were not reported (Offermanns et al., 1998). $G\alpha_{13}$ (gene symbol *Gna13*) is an important GPCR effector in endothelial cells and neural crest during embryonic development, and $G\alpha_{13}$ signaling in neural crest contributes to neural tube closure (Ruppel et al., 2005). To determine whether $G\alpha_{13}$ in surface ectoderm might also contribute to neural tube closure, we generated surface ectoderm-specific *Gα13* knockouts. *Grhl3*$^{Cre/+}$:*Gα13*$^{f/f}$ embryos lived through E14.5 and did not display exencephaly. Addressing possible redundancy with $G\alpha_{12}$, we found that *Grhl3*$^{Cre/+}$:*Gα13*$^{f/f}$:*Gα12*$^{-/-}$ embryos died by E10.5 with turning and other defects but with a closed hindbrain neuropore (not shown). Thus, loss of $G\alpha_{12/13}$ signaling in surface ectoderm is unlikely to account for exencephaly in *Par1*$^{-/-}$:*Par2*$^{-/-}$ embryos.

We next addressed the role of the $G_{i/o/z}$ family. Four of the five widely expressed $G\alpha_{i/o/z}$ family members ($G\alpha_{i1}$, $G\alpha_{i2}$, $G\alpha_{i3}$, and $G\alpha_o$) are inhibited by pertussis toxin; $G\alpha_z$ is pertussis-insensitive. To circumvent redundancy among the $G\alpha_{i/o/z}$ family members, we used a *ROSA26*^{PTX} conditional allele (Regard et al., 2007) to express pertussis toxin S1 catalytic subunit (PTX) in surface ectoderm by Cre-mediated excision of a Lox-Stop-Lox cassette. Embryos from *ROSA26*$^{PTX/PTX}$ × *Grhl3*$^{Cre/+}$ crosses were collected at 14.5 dpc. *Grhl3*$^{Cre/+}$:*ROSA26*$^{PTX/+}$ embryos showed exencephaly with a penetrance of ~10% (Figure 3). The frequency of exencephaly increased to 20% in a $G\alpha_z$ null background. Exencephaly was not observed in mice lacking only $G\alpha_z$ nor in Cre-negative *ROSA26*$^{PTX/+}$:$G\alpha_z^{-/-}$ embryos. Posterior neural tube defects — spina bifida and curly tail — were seen in 0%, 18%, and 40% of *Grhl3*$^{Cre/+}$:*ROSA26*$^{PTX/+}$ embryos in $G\alpha_z^{+/+}$, $^{+/-}$ and $^{-/-}$ backgrounds, respectively. Thus, PTX S1 expression in surface ectoderm and $G\alpha_z$ deficiency interacted to promote neural tube defects, strongly supporting the notion that these phenotypes are caused by loss of $G_{i/o/z}$ pathway function and hence that G_i signaling in surface ectoderm is required for normal closure of the neural tube. In contrast to *Grhl3*$^{Cre/+}$:*ROSA26*$^{PTX/+}$:$G\alpha_z^{-/-}$ embryos, posterior neural tube defects were rare in *Par1*$^{-/-}$:*Par2*$^{-/-}$ embryos. Grhl3 expression in hindgut contributes to posterior neuropore closure (Gustavsson et al., 2007). Although neural tube defects were not detected in *Grhl3*$^{Cre/+}$ embryos, it is possible that haploinsufficiency of Grhl3 interacts with loss of Gi signaling in hindgut in *Grhl3*$^{Cre/+}$:*ROSA26*$^{PTX/+}$:$G\alpha_z^{-/-}$ embryos to produce such defects. It is also possible that knockout of Gi pathway signaling uncovered a role for G_i-coupled GPCRs in addition to Par2 and Par1 in posterior neural tube closure.

Rac is one of several downstream effectors of G_i signaling. Abrogation of Rac function impairs dorsal closure of the Drosophila embryo cuticle due to an inability of opposing epithelial sheets to migrate and fuse (Harden et al., 1995). Rac1 is the main Rac family member expressed in non-hematopoietic tissues in mice (Sugihara et al., 1998). To determine whether Rac function in surface ectoderm might be necessary for neural tube closure in mouse embryos, we examined

Grhl3$^{Cre/+}$:*Rac1*$^{f/f}$ embryos collected at 14.5 dpc (Figure 3). 58% of *Grhl3*$^{Cre/+}$:*Rac1*$^{f/f}$ embryos displayed exencephaly vs. 0% for Cre-negative Rac1$^{f/f}$ embryos or Cre-positive embryos with a single wild-type Rac1 allele (Figure 3). As with elimination of $G_{i/o/z}$ function in surface ectoderm, we also observed posterior neural tube defects at a high rate (83%). *Grhl3*$^{Cre/+}$:*Rac1*$^{f/f}$ embryos were present at the expected Mendelian frequency, and X-gal staining (for β-gal expressed from the IRESlacZ included with the *Grhl3* Cre knockin) demonstrated that most surface ectoderm cells expressed Cre at this time. Thus, Rac1 function was not required for survival of surface ectoderm cells. These results are consistent with a model in which Gi-Rac signaling downstream of PARs and other GPCRs in surface ectoderm contributes to neural tube closure.

Neural tube defects are often classified as sensitive or resistant to folate supplementation (Copp et al., 2003). Folate injections of pregnant female mice (Fleming and Copp, 1998) at E7.5 and 8.5 did not affect the penetrance of hindbrain or posterior neural tube defects in *Grhl3*$^{Cre/+}$:*Rac1*$^{f/f}$ embryos collected at 14.5 dpc (Figure 3), suggesting that these defects are folate-resistant.

Identification of candidate Par2-activating proteases in the context of neural tube closure

Multiple serine proteases can activate Par2 in vitro but its physiological activators are uncertain. Uncovering a necessary role for surface ectoderm Par2 in neural tube closure provided a context in which to search for a Par2-activating protease. Toward identifying candidate proteases, we first asked which extracellular proteases are expressed in the mouse embryo at the time of neural tube closure and which proteases are expressed in tissues in a pattern most like Par2.

We generated TaqMan-type qPCR primer/probe sets for the ~125 genes in mouse predicted to encode a serine protease that would reside in the extracellular compartment (e.g., proteases with signal peptides, or type-2 transmembrane proteins with extracellular protease domain (TTSPs); Document S2) and used these to quantitate mRNAs in mouse embryos collected at 8.5–9.5 dpc. About 25% of the 125 protease genes examined were expressed above background. We focused first on the ten most abundantly expressed (Figure 4A), especially in light of our cluster results (see below). Analysis of RNA from FACS-sorted surface ectoderm cells from *Grhl3*$^{Cre/+}$:ROSA26$^{YFP/+}$ embryos collected at 8.5–9.5 dpc confirmed expression of nine of these ten in surface ectoderm, and mRNA for four proteases — prostasin, epitheliasin, matriptase (also known as MT-SP1 and St14), and hepsin — was enriched in surface ectoderm relative to the rest of the embryo (Figure 4A).

Cluster analysis of the pattern of expression of the 125 proteases and 11 selected inhibitors across 44 different tissues in adult mice revealed matriptase (St14) and prostasin (Prss8), their Kunitz-type inhibitors Hai-1 and Hai-2 (Spint1 and 2), and epitheliasin (Tmprss2) to be expressed in a pattern most similar to Par2 (F2rl1) (Figure 4B and Document S3). Hepsin was broadly expressed and did not specifically cluster with Par2, but hepsin and Par2 were often expressed in the same tissues. Prostasin, matriptase, hepsin, and epitheliasin are membrane-tethered proteases and hence are likely to function on or near the cell in which they are expressed. These results raised the possibility that matriptase, prostasin, hepsin and/or epitheliasin might, together with Par2, comprise a local protease signaling system in surface ectoderm. Our previous observation that matriptase can activate Par2 heterologously expressed in Xenopus oocytes (Takeuchi et al., 2000) encouraged investigation of this hypothesis.

In situ hybridization confirmed expression of prostasin, epitheliasin, matriptase, and hepsin mRNA in surface ectoderm of wild-type embryos collected at 8.75 dpc; t-PA and Klk8 hybridization was also detected and was more widespread (Figure 4C). Although Masp1 was expressed in surface ectoderm (Figure 4A), past studies had suggested that Masp1 was not an

effective Par2 activator (not shown). Based on these results, we chose Klk8, prostasin, tPA, epitheliasin, matriptase and hepsin for further study.

Par2 cleavage and signaling in response to candidate proteases

To determine whether these proteases might elicit signaling in cells that express Par2 at natural levels, we examined phosphoinositide (PI) hydrolysis in response to exogenous soluble recombinant proteases added to cultures of HaCaT cells, a keratinocyte-like surface ectoderm lineage cell line that naturally expresses PAR1 and PAR2. At 50 nM, prostasin, matriptase, and hepsin protease domains triggered PI hydrolysis in HaCaT cells; Klk8, t-PA and epitheliasin had no activity (Figure 5A). Matriptase was remarkably potent in the HaCaT system, with an EC_{50} of ~200 pM; EC_{50} values for prostasin and hepsin were around 20 nM (Figure 5B). Responses were blocked by recombinant ecotin or HAI-1 (not shown), both broad-spectrum inhibitors of trypsin-fold serine proteases (Takeuchi et al., 1999), confirming that responses to the recombinant protease preparations were indeed due to protease activity.

To assess the ability of proteases to productively cleave individual PARs, we transiently transfected HaCaT cells with Par1 and Par2 that had alkaline phosphatase (AP) fused to their N-terminal exodomains such that receptor cleavage released alkaline phosphatase into the culture medium (Ludeman et al., 2004). Addition of 10 nM soluble recombinant matriptase to HaCaT cultures expressing AP-Par2 released 90–95% of surface-available (trypsin-releasable) AP within 60 minutes in 3 of 3 separate experiments, 20–60% was released by 10–20 nM prostasin, and hepsin showed some but variable activity in this assay (Figure 5C and Figure S5, S6). None of these proteases released AP activity from cells expressing AP-Par2csm, an AP-Par2 mutant with a two amino acid change that disrupts its activating cleavage site (Figure S5). Thus, exposure to matriptase, prostasin, and hepsin resulted in productive cleavage of Par2 expressed in HaCaT cells.

Unlike AP-Par2, AP release from AP-Par1-transfected HaCaT cells by recombinant matriptase, prostasin, and hepsin was not ablated by mutation of the activating cleavage site in Par1 (not shown). Par1 is subject to nonproductive cleavage and shedding of its N-terminal exodomain by an ADAM17-like metalloproteinase (Ludeman et al., 2004), and prostasin, hepsin and matriptase failed to cause AP release from AP-Par1-transfected HaCaT cells in the presence of the metalloproteinase inhibitor 1,10-phenanthroline (Figure S5). AP release from AP-Par2-transfected cells upon addition of prostasin, hepsin and matriptase was unaffected by metalloproteinase inhibition (Figure S5). Metalloproteinase-dependent Par1 shedding can be increased by stimulation of protein kinase C (Ludeman et al., 2004). Thus, PAR2 activation of metalloproteinase-dependent Par1 shedding may account for release of AP from AP-Par1 by matriptase, prostasin, and hepsin in the HaCaT system in the absence of metalloproteinase inhibition.

Evidence for a Par2-activating protease “cascade”

The experiments described above do not speak to whether matriptase, prostasin, and/or hepsin act upon Par2 directly. Toward addressing this question, we first examined the ability of these proteases to trigger Par2 transfection-dependent PI hydrolysis in lung fibroblasts from Par1-deficient mice (KOLF). In the absence of transfection, KOLF do not express Par2 or other PARs, matriptase, prostasin, hepsin or Hai-1 mRNA as assessed by TaqMan RT-PCR. In accord, even at 50 nM, exogenous matriptase, prostasin, and hepsin did not stimulate PI hydrolysis in untransfected KOLFs (Figure 5D). After PAR2 transfection of KOLFs, matriptase triggered signaling as effectively as saturating concentrations of PAR2 agonist peptide and with an EC_{50} of ~300 pM (Figure 5D,E), similar to that found in HaCaT cultures (Figure 6B). Matriptase showed no activity in PAR1- or PAR4-transfected KOLFs even at >100x the EC_{50} for PAR2 (Figure 5D and not shown). Similar results were obtained whether

mouse or human PAR cDNAs were transfected. Activity at PAR3 was not examined because the mouse homolog of this receptor is incapable of mediating transmembrane signaling (Nakanishi-Matsui et al., 2000).

Surprisingly, in contrast to the case in HaCaT cells, prostasin produced no PI hydrolysis response in KOLFs transfected to express PAR2 or other PARs (Figure 5D and not shown). Similarly, only a weak response to hepsin was detected (Figure 5D,E). The different protease responsiveness of HaCaT and KOLF cultures suggested that KOLFs might lack a factor that permits, or express an inhibitor that prevents, direct or indirect PAR2 activation by prostasin and hepsin. Quantitative PCR analysis showed that matriptase was expressed by HaCaTs but not by KOLFs. This and the potency of matriptase as a PAR2 activator suggested that activation of the zymogen form of matriptase by prostasin or hepsin might account for the ability of these proteases to activate PAR2 in HaCaT cultures. To test this possibility, we first determined whether matriptase inhibition would attenuate signaling in response to prostasin and hepsin in HaCaT cultures.

E2, a potent and highly selective antibody inhibitor to matriptase (Farady et al., 2008; Sun et al., 2003), blocked the ability of prostasin and hepsin to trigger phosphoinositide hydrolysis in HaCaT cultures (Figure 6A). E2 at the same concentration had no effect on signaling by factor Xa (Figure 6A), which can directly activate PAR2, nor did E2 inhibit the activity of 10nM prostasin or hepsin in amidolytic assays (not shown). These results suggested that prostasin and hepsin activated Par2 in HaCaTs by an indirect mechanism that was matriptase-dependent. To further probe this possibility, we examined Par2 cleavage in KOLFs with and without co-expression of matriptase. Hai-1 was co-expressed with matriptase in these experiments because matriptase expression in the absence of its inhibitor appeared to be toxic (not shown). In contrast to soluble recombinant matriptase, addition of soluble recombinant prostasin to KOLFs expressing AP-Par2 or AP-Par2 plus Hai-1 did not trigger AP release. However, soluble recombinant prostasin did release AP from KOLFs expressing AP-Par2 and Hai-1 plus matriptase but not active site mutant matriptase nor a matriptase mutated at the site required for proteolytic processing of the matriptase zymogen to the active form (Figure 6B and S6). Thus, Par2 cleavage by prostasin required expression of matriptase with an intact active site and an intact zymogen conversion site, consistent with a model in which prostasin activates Par2 by activating matriptase zymogen co-expressed in the same or nearby cells. Similar results were obtained with hepsin, but hepsin also showed weak direct activity at Par2 (Figure S6).

Purified recombinant matriptase can spontaneously cleave itself from zymogen to active form (Takeuchi et al., 1999), but how matriptase is activated in vivo and how such activation is regulated is unknown. To probe the state of matriptase heterologously expressed in KOLFs and naturally expressed in HaCaT cells and to further test the model that such matriptase can be activated by prostasin and hepsin, we utilized specific antibodies that distinguish two-chain, active matriptase from its zymogen form (Benaud et al., 2001; Wang et al., 2009). The fact that active matriptase migrates in a complex with Hai1 on non-reducing SDS-PAGE was also exploited to detect formation of active matriptase (Oberst et al., 2003).

Lysates of KOLFs transfected with Hai-1 plus vector or matriptase were analyzed by immunoblot with M69 and M24 antibodies; M69 recognizes the processed active form and M24 recognizes both zymogen and active forms (Wang et al., 2009). In the absence of added protease, matriptase and Hai-1 co-transfection resulted in the appearance of a 70 kDa band recognized by M24 but not M69, consistent with expression of matriptase in its zymogen form (Figure 6C, lane 4). Treatment with soluble recombinant active matriptase, prostasin, or hepsin caused the appearance of a matriptase transfection-dependent ~120 kDa band recognized by M69, consistent with appearance of active matriptase complexed with Hai-1 (Figure 6C, lanes

5–7). Prostasin was consistently the most active in this regard. The intensity of the 70kDa zymogen band recognized by M24 was concomitantly decreased, consistent with conversion of matriptase zymogen to its active form. The 65kDa band in the M69 blots likely represents the truncated soluble recombinant matriptase, which is not recognized by M24. Exogenous matriptase, prostasin, and hepsin treatment also converted a matriptase active site mutant to a form recognized by M69 and Hai-1, suggesting that matriptase activity and autoactivation are not required to convert matriptase from its zymogen to its two-chain form in this system (Figure 6C, lanes 9–11). These results are consistent with a model in which prostasin and hepsin cleave and convert matriptase zymogen expressed on the surface of KOLFs to its active form.

Similar results were obtained in HaCaT cells that naturally express matriptase and HAI1. In lysates of untreated HaCaTs, matriptase was mainly in the zymogen form (Figure 6D, lanes 1–2, ~70 kDa band in M24 panel). Addition of soluble recombinant active matriptase, prostasin or hepsin caused the appearance of the active form of matriptase migrating in complex with Hai-1 (Figure 6D, lanes 3–8, ~120 kDa band in M69 panel). This band was also recognized by Hai-1 immunoblot (not shown). Again, prostasin was the most active of the three proteases tested in this assay. Taken together, our results are consistent with the notion that prostasin and hepsin activate the zymogen form of matriptase on KOLF and HaCaT cells.

Evidence for the presence of active matriptase at the time and place of neural tube closure

The results outlined above suggest a model in which matriptase and Par2 are co-expressed in the surface ectoderm, with matriptase becoming activated locally in a manner that activates Par2 and supports normal closure of the neural tube. Matriptase is co-expressed with its inhibitors, Hai1 and 2 (Figure 4; see also (Kirchhofer et al., 2003;List et al., 2005;Szabo et al., 2008)), and with its candidate activators prostasin and hepsin. When and where active matriptase is made available to cleave substrates in vivo is unknown (List et al., 2006). To determine whether active matriptase is present at the same time and place as Par2 during neural tube closure, we utilized E2 (Farady et al., 2008) conjugated to Alexafluor 594 to stain live mouse embryos collected at 8.5 dpc (Figure 4D and Figure S5). Antibody bound to surface ectoderm in a distribution similar to that of Par2 expression. A control fluorescently labeled antibody showed no such anatomically specific binding. These results suggest that the matriptase active site is present on surface ectoderm cells at the time and place of neural tube closure, consistent with the model described above.

Discussion

PARs function in the context of responses to injury in the adult and contribute to cardiovascular development in the embryo. Our results show an unexpected role for PARs and protease signaling in regulating neural tube closure in the mouse embryo. Our results also suggest that matriptase and other membrane-tethered proteases co-expressed with Par2 may comprise a local protease network that activates Par2 in this context. This paradigm for autocrine/paracrine PAR activation raises interesting questions regarding the roles of local protease signaling in regulating epithelia, and the observation that Par2 and other Gi-coupled GPCRs in surface ectoderm contribute to neural tube closure in mice may lead to insights into the complex mechanisms underlying human neural tube defects.

A role for PARs and Gi signaling in neural tube closure

During neural tube closure in rodents, surface ectoderm is the first structure to close the gap between the opposing sides of the open neural tube at the level of the hindbrain neuropore; at most other levels, the neuroepithelium is the site of initial closure (Geelen and Langman, 1979; Waterman, 1976). Exencephaly in *Par1*$^{-/-}$:*Par2*$^{-/-}$, *Grhl3*$^{Cre/+}$:*ROSA26*$^{PTX/+}$, and *Grhl3*$^{Cre/+}$:*Rac1*$^{f/f}$ embryos suggests that disruption of GPCR, G_i, and Rac1 signaling in

surface ectoderm hampers neural tube closure where surface ectoderm closure is an early event, but posterior neural tube defects in *Grhl3*$^{Cre/+}$:*ROSA26*$^{PTX/+}$ and *Grhl3*$^{Cre/+}$:*Rac1*$^{f/f}$ embryos suggest that Gi pathway signaling in surface ectoderm also contributes where the surface ectoderm closes after the neuroepithelium. Events during neural tube closure include fusion of the neuroepithelium, fusion of the surface ectoderm, de-adhesion of the neuroepithelium from the surface ectoderm and separation of the closed ectoderm from the neural tube, differentiation and migration of neural crest cells between these structures, and extensive remodeling of the extracellular matrix (Geelen and Langman, 1979; Greene and Copp, 2009; Schoenwolf and Smith, 1990; Waterman, 1976; Zohn and Sarkar, 2008). Par2, G_i and Rac regulate multiple cellular events including reorganization of the actin cytoskeleton, lamellipod formation, cell spreading, polarization and migration, integrin and cadherin function, and other cellular processes. Which of these accounts for the phenotypes described herein remains to be determined.

The similarity of the *Grhl3* and *Par2* expression patterns prompted us to use *Grhl3* to drive Cre recombinase expression for surface ectoderm-specific excision of floxed alleles. Intriguingly, the 5′ region of *Par2* contains several potential Grhl3 binding sites. Gel shift assays confirmed that these sites bind protein in a sequence-specific manner, but decreased *Par2* expression in surface ectoderm was not detected in *Grhl3* nulls (not shown). Whether *Grhl3* participates in the control of *Par2* expression and whether and how these genes might interact to contribute to neural tube closure remains to be determined. Regardless, Grhl3-Cre should be useful for excision of floxed alleles selectively in surface ectoderm.

Candidate Par2-activating proteases during neural tube closure

The finding that Par2 contributes to neural tube closure raised the question of what this receptor senses biochemically and physiologically. An answer requires identifying the protease(s) that activates Par2 in this context. Proteases reproducibly shown to cleave PARs productively have been extracellular serine proteases. Accordingly, we focused on secreted, GPI-linked, and integral membrane proteins with an extracellular serine protease domain that are expressed in embryos at the time of neural tube closure as candidate Par2 activators. Analysis of Par2 and protease expression patterns, abundance in embryos collected at 8.5–9.25 dpc, expression in surface ectoderm at this time, and functional testing all pointed to matriptase as a strong candidate Par2 activator during neural tube closure.

Matriptase is a type-2 transmembrane protein with a serine protease domain at its extracellular carboxyl terminal. We previously identified matriptase as a potential Par2 activator based on its P1-P4 substrate sequence preference and found that recombinant matriptase protease domain activated Par2 heterologously expressed in Xenopus oocytes (Takeuchi et al., 2000). However, the EC_{50} for Par2-dependent signaling in this system was relatively high (>10 nM), and there was no obvious context in which to determine whether matriptase was a physiological Par2 activator. In the current study, recombinant matriptase productively cleaved and activated Par2 expressed in mammalian cells with an EC_{50} in the 200–300 pM range. Whether the difference in EC_{50}s in the Xenopus and mammalian systems is due to differences in temperature (25 vs. 37 °C), protease inhibitors, or other factors is unknown. Regardless, the impressive potency of soluble recombinant matriptase for Par2 activation in mammalian cells and the fact that the matriptase protease domain is normally tethered to the cell surface suggests that matriptase might be a physiological activator of Par2 in cells that express both protease and receptor. Detection of matriptase mRNA in surface ectoderm (Figure 4A,C) and binding of a matriptase active site-specific antibody to the surface ectoderm cells near the closing neural tube (Figures 4C and S4) suggests that active matriptase may indeed co-exist with Par2 in vivo at a place and time consistent with a role in neural tube closure.

Matriptase did not show agonist activity for Par1, and the protease(s) that might activate Par1 in its possible back-up role in neural tube closure is unknown. No neural tube defects were reported in the matriptase knockout mice (List et al., 2002), but none would be expected if Par1 were activated by a matriptase-independent mechanism.

A local network of membrane-tethered proteases may trigger Par2 signaling

Several observations suggest that prostasin, which is GPI-linked to the cell surface, might interact with matriptase and contribute to Par2 activation. Prostasin is co-expressed with matriptase as well as Hai-1 and Hai-2, Kunitz-type inhibitors for both proteases, in many tissues (List et al., 2007) including surface ectoderm at the time of neural tube closure (Figure 4), and knockouts of the prostasin and matriptase genes in mouse exhibit similar phenotypes (defective skin development and barrier function) (Leyvraz et al., 2005; List et al., 2002). Both proteases are also tightly co-expressed with Par2 (Figure 5 and (Bhatt et al., 2007)). While soluble recombinant matriptase appeared to activate Par2 directly, soluble recombinant prostasin activated Par2 indirectly by a matriptase-dependent mechanism (Figures 5 and 6). The simplest model consistent with these and other data is that prostasin converts matriptase from a zymogen form to an active form that can in turn activate Par2. In accord with this model, we recently observed that, like loss of matriptase inhibition (Szabo et al., 2009b), overexpression of either proprostasin or Par2 in mouse skin led to ichthyosis and that Par2 deficiency rescued skin abnormalities caused by prostasin overexpression (Frateschi S, Camerer E, Coughlin SR, Hummler E and colleagues, submitted for publication). Par2 dependence of matriptase gain-of-function phenotypes was not addressed (Szabo et al., 2009b).

Although hepsin was expressed more broadly than matriptase, prostasin and Par2, it was expressed in surface ectoderm during neural tube closure, and, like prostasin, a soluble recombinant hepsin that included its protease domain showed matriptase-dependent signaling activity (Figure 5, 6). Hepsin is a type-2 transmembrane protein with an extracellular protease domain, and cell surface-localized hepsin might well be an effective matriptase activator.

Epitheliasin, another type-2 transmembrane protein with an extracellular protease domain that was expressed in surface ectoderm during neural tube closure, was often co-expressed with matriptase and Par2 (Figure 4). We did not detect epitheliasin-triggered signaling activity in either HaCaTs or matriptase and PAR2-expressing KOLFs, but PAR2-dependent signaling in LNCaP cells has been reported (Wilson et al., 2005). Epitheliasin might use an indirect mechanism to activate PAR2 in LNCaP cells that requires components present in LNCaP cells but absent in the HaCaT and KOLF systems.

Consistent with the mechanism proposed above for matriptase-dependent Par2 activation by prostasin, our data suggest that matriptase naturally expressed in HaCaT s or co-expressed with Hai-1 in KOLFs exists predominantly in the zymogen form and is converted to the active form upon addition of active prostasin or hepsin (Figure 6C,D). Thus, Par2 activation in surface ectoderm cells that also express matriptase might be regulated at the level of matriptase activation. How matriptase activation is regulated in vivo is unknown. While our results suggest that prostasin can activate matriptase, there is strong evidence that matriptase is necessary for normal prostasin activation, at least in skin (Netzel-Arnett et al., 2006). Together, these observations raise the possibility that prostasin might function both downstream and upstream of matriptase to constitute a positive feedback loop. Ready examples of this paradigm exist in the coagulation cascade, in which the effector protease thrombin activates upstream coagulation factors that mediate thrombin generation to amplify thrombin production and propagate coagulation in space and time (Broze, 1995).

Possible physiological roles for membrane-tethered protease/Par2 signaling

Intriguingly, while matriptase and prostasin are often expressed in the same epithelial cell, they may sort to distinct membrane compartments, with matriptase directed basolaterally and prostasin apically (Godiksen et al., 2008; Wang et al., 2009). Could it be that a prostasin-matriptase-Par2 network has evolved to sense breaks in epithelial barrier function, in which loss of cell-cell junctions allows mixing of compartments such that the proteases make contact, activate and trigger activation of Par2 and other effectors? And/or might this system function at the edges of closing epithelial sheets or in immature epithelium, where junctions and apical-basal polarity have not yet been established such that protease interaction and activation is permitted? Our detection of active matriptase predominantly at the edges of the surface ectoderm during neural tube closure is consistent with models that include such localized protease activation.

It was recently reported that deficiency of the protease inhibitor Hai-2 causes neural tube closure defects in mouse embryos that were partially rescued by concomitant matriptase deficiency (Szabo et al., 2009). If matriptase activates Par2, how might matriptase gain-of-function and Par2 loss-of-function yield similar phenotypes? Gain of matriptase function might result in increased cleavage of other physiological substrates and/or cleavage of non-physiological substrates to disrupt neural tube closure by a mechanism unrelated to Par2 activation. Alternatively, loss of matriptase inhibition might disrupt normal spatial and temporal control of Par2 activation and/or excess matriptase activity might downregulate Par2, effectively causing loss of Par2 function. Either mechanism might disrupt the precise tissue remodeling that occurs during neural tube closure (Massa et al., 2009). Regardless, this report supports the notion that matriptase is normally expressed and active in or around the closing neural tube, consistent with the model outlined above.

Might the paradigm of membrane-tethered or locally secreted proteases acting via Par2 to regulate epithelial function extend beyond neural tube closure? Expression profiling confirms a tight link in expression of Par2, matriptase, prostasin, and epitheliasin across epithelial organs in adult mice, suggesting a potential functional link in adult biology as well. There are several reported roles for these proteases in regulating external barriers and in tumor progression where Par2 might be explored as a candidate effector (Bhatt et al., 2007; Klezovitch et al., 2004; Leyvraz et al., 2005; List et al., 2002; List et al., 2009; List et al., 2005). Like prostasin and matriptase, overexpression of Par2 in skin leads to hyperkeratosis, stratum corneum detachment and itching (EC and SRC, unpublished observations). Similar phenotypes have been reported for overexpression of Klk7 (Hansson et al., 2002), and excessive Klk5 activity secondary to loss of Kazal-type related inhibitor (LektI; encoded by the Spink5 gene) has been suggested to drive stratum corneum detachment in Netherton syndrome in a PAR2-dependent manner (Briot et al., 2009). KLK5 has been reported as a PAR2 activator (Oikonomopoulou et al., 2006); we have confirmed this finding, whereas KLK7 appears to induce matriptase-dependent activation of Par2 like prostasin (not shown). PAR2 has a complex role in inflammation in the gastrointestinal tract (Vergnolle, 2000); tryptase, trypsin and Xa have been proposed activators in this context, but type-2 transmembrane serine proteases are highly expressed in gut epithelium and might well play a role. Together with our results, these observations support exploration of the notion that local networks of membrane-tethered proteases and Par2 might contribute to the regulation of epithelial function in homeostasis and disease.

Experimental Procedures

Nomenclature

Gene names are italicized. Human genes and proteins are in capital letters (*ST14*, ST14); mouse has first letter capitalized (*St14*, St14). Protease-activated receptors are designated by their commonly used designation Par1, Par2, etc. (their HUGO gene names are F2r, F2rl1, etc.). PARs is used to refer to the family generically. Genes encoding Grhl3; the G protein α subunits $G\alpha_{12}$, $G\alpha_{13}$, and $G\alpha_z$; and matriptase are designated *Grhl3; $G\alpha_{12}$, $G\alpha_{13}$, and $G\alpha_z$*; and *St14*, respectively. HUGO gene names for $G\alpha_{12}$, $G\alpha_{13}$, and $G\alpha_z$ are *Gna12, Gna13 and Gnaz*, respectively.

Mice, timed matings and gross analysis of mouse embryos

Experiments were performed in accordance with protocols approved by the UCSF internal animal use and care committee. Generation of mutant mice is described in Supplemental Experimental Procedures (Document S1). The morning a vaginal plug was detected was considered 0.5 days post coitus (dpc). For embryo collection, yolk sack and placenta were removed intact, scored as below, then embryos were removed, examined and photographed. Before 12.5 dpc, viability was scored by the presence or absence of a heartbeat. At or after 12.5, the presence of pulsation in vitelline or umbilical vessels or response to pinch was used. In some cases, embryos and deciduas were fixed en bloc and processed for paraffin embedding and sectioning.

X-gal staining and in situ hybridization

Embryos were fixed, processed for X-gal staining (Document S1)(Griffin et al., 2001), then imaged or paraffin embedded, sectioned at 5 μm and counterstained with Nuclear Fast Red. For in situ hybridization, 9.0 dpc embryos were fixed in 4% paraformaldehyde, washed and dehydrated. In situ hybridization was performed in whole mount or on 5 μm paraffin sections (Henrique et al., 1995; Soifer et al., 1994); images were acquired as in Document S1.

Cell Culture and cell signaling assays

HaCaTs and vector- and PAR-transfected KOLFs were grown in DMEM with 10% FBS, 100 units/ml penicillin, and 100 μg/ml streptomycin (Camerer et al., 2000). KOLF, $KOLF_{PAR2}$ or HaCaTs were transiently transfected with pSPORT6 (Open Biosystems) and pCDNA3 (Invitrogen) expression vectors carrying cDNAs for matriptase, $matriptase_{S805A}$, Hai-1 and/or human or mouse PARs by electroporation (Amaxa Inc) or using Mirus transfection reagent (Mirus). The next day, the cells were washed and incubated in SFM (serum-free DMEM with 20 mM HEPES and 0.1% bovine serum albumin (BSA)) with 2 μCi/mL *myo*-[^{3}H]inositol overnight, then washed again and incubated with SFM for 2 hours prior to the addition of agonist and LiCl for 90 minutes. Cells were then extracted and released inositol phosphates measured (Camerer et al., 2000).

Receptor cleavage assay

AP-*Par1* and AP-*Par2* encoding secreted human placental alkaline phosphatase (SEAP) fused to the mouse PAR N-terminal with an intervening linker region containing the FLAG epitope were generated (Ludeman et al., 2004). Briefly, the coding regions of *Par1* and *Par2* C-terminal to the signal peptidase site were PCR amplified and ligated into the HpaI (5′) and XbaI (3′) sites of pCMV-SEAP (Tropix/Applied Biosystems) such that the SEAP stop codon was removed and SEAP was joined to each Par via an SGASGA linker. PCR-based site directed mutagenesis was used to generate $Par2_{R38A/S39P}$ and $Par1_{R41A/S42P}$ cleavage site mutants and to generate the $matriptase_{S805A}$ in which the active site serine was replaced by alanine (Takeuchi et al., 1999).

KOLF and HaCaT cells were transiently transfected with human or mouse matriptase, matriptase$_{S805A}$, and/or Hai-1 together with AP-Par1 or AP-Par2 or their cleavage site mutants. The next day, cells were washed and incubated in serum-free M199 with 25 mM HEPES and 0.1% BSA for two hours, treated with the indicated proteases for 60 minutes, and conditioned medium was assayed for alkaline phosphatase activity (Ludeman et al., 2004). The amount of intact receptor remaining on the cell surface and still available for cleavage after treatment with test proteases was determined by washing cells, then treating with trypsin (50 nM; Sigma) for an additional 5 minutes, at which time conditioned medium was collected and AP again measured. Data is presented as fold increase or % of total AP released (AP released by test protease/(same + remaining surface AP released by trypsin)). For HaCaT cell studies, 1,10 phenanthroline (5 mM) was added to the incubation medium to inhibit metalloprotease-dependent non-productive PAR shedding (Ludeman et al., 2004).

Matriptase immunoblot

Cells were treated as indicated, washed twice with ice-cold Tris-buffered saline (TBS) then lysed in 1X Laemmli sample buffer. Lysates were analyzed by SDS/PAGE under non-boiling, non-reducing conditions, then blotted onto nitrocellulose membranes. Membranes were incubated with mouse monoclonal antibodies for active (M69) or total (M24) matriptase (Wang et al., 2009), then with horseradish peroxidase-conjugated goat anti-mouse IgG (Invitrogen) and chemiluminescence detection reagents (GE Healthcare).

Statistical analysis

Phenotype frequencies were analyzed by Chi-Square. Phosphoinositide hydrolysis and AP release assays were analyzed by one- or two-way ANOVA followed by t-test for individual comparisons. Bonferroni correction for planned multiple comparisons was included when appropriate. Single, double and triple asterisks (*) indicate $p<0.05$, 0.01 and 0.001 compared to vehicle control, respectively; not significant (ns) indicates $p>0.05$. The findings reported in Figures 5 and 6 were reproduced at least twice. Data shown are mean +/- SD. N was 3 or greater except for 6B (n=2).

Additional methods

Please refer to Document S1 for generation of mutant mice, protease database, qPCR array and analysis, E2 immunostaining of embryos for active matriptase, and additional methods.

Supplementary Material

Refer to Web version on PubMed Central for supplementary material.

Acknowledgments

S.R.C., C.S.C. and co-workers are funded by the National Institutes of Health. Eric Camerer is funded by an INSERM Avenir Fellowship. Daniel Kirchhofer and Rajkumar Ganesan are employees of Genentech, Inc. Linda Prentice, Lydia-Marie Joubert, Jinny Wong, Leonor Patel, Cherry Concengco, Khushboo Kaushal, Ganesh Elongavan, and Jay Dietrich for technical support; Brian Black, Orion Weiner, Takashi Mikawa, Sarah DeVal, Pooja Agarwal for advice; Nirao Shah for the IRES-NLSlacZ construct; Mel Simon, Skip Brass, David Kwiatkowski, Jun-ichi Miyazaki, Nigel Killeen and Susan Dymecki for mouse lines; and Henry Bourne for critical reading of the manuscript.

References

Auden A, Caddy J, Wilanowski T, Ting SB, Cunningham JM, Jane SM. Spatial and temporal expression of the Grainyhead-like transcription factor family during murine development. Gene Expr Patterns 2006;6:964–970. [PubMed: 16831572]

Becker RC, Moliterno DJ, Jennings LK, Pieper KS, Pei J, Niederman A, Ziada KM, Berman G, Strony J, Joseph D, et al. Safety and tolerability of SCH 530348 in patients undergoing non-urgent percutaneous coronary intervention: a randomised, double-blind, placebo-controlled phase II study. Lancet 2009;373:919–928. [PubMed: 19286091]

Benaud C, Dickson RB, Lin CY. Regulation of the activity of matriptase on epithelial cell surfaces by a blood-derived factor. Eur J Biochem 2001;268:1439–1447. [PubMed: 11231297]

Bhatt AS, Welm A, Farady CJ, Vasquez M, Wilson K, Craik CS. Coordinate expression and functional profiling identify an extracellular proteolytic signaling pathway. Proc Natl Acad Sci U S A 2007;104:5771–5776. [PubMed: 17389401]

Briot A, Deraison C, Lacroix M, Bonnart C, Robin A, Besson C, Dubus P, Hovnanian A. Kallikrein 5 induces atopic dermatitis-like lesions through PAR2-mediated thymic stromal lymphopoietin expression in Netherton syndrome. J Exp Med 2009;206:1135–1147. [PubMed: 19414552]

Broze GJ Jr. Tissue factor pathway inhibitor and the revised theory of coagulation. Annu Rev Med 1995;46:103–112. [PubMed: 7598447]

Camerer E, Duong DN, Hamilton JR, Coughlin SR. Combined deficiency of protease-activated receptor-4 and fibrinogen recapitulates the hemostatic defect but not the embryonic lethality of prothrombin deficiency. Blood 2004;103:152–154. [PubMed: 14504091]

Camerer E, Huang W, Coughlin SR. Tissue factor- and factor X-dependent activation of protease-activated receptor 2 by factor VIIa. Proc Natl Acad Sci U S A 2000;97:5255–5260. [PubMed: 10805786]

Camerer E, Kataoka H, Kahn M, Lease K, Coughlin SR. Genetic evidence that protease-activated receptors mediate factor Xa signaling in endothelial cells. J Biol Chem 2002;277:16081–16087. [PubMed: 11850418]

Connolly AJ, Ishihara H, Kahn ML, Farese RV Jr, Coughlin SR. Role of the thrombin receptor in development and evidence for a second receptor. Nature 1996;381:516–519. [PubMed: 8632823]

Copp AJ, Greene ND, Murdoch JN. The genetic basis of mammalian neurulation. Nat Rev Genet 2003;4:784–793. [PubMed: 13679871]

Coughlin SR. Thrombin signalling and protease-activated receptors. Nature 2000;407:258–264. [PubMed: 11001069]

Coughlin SR, Camerer E. PARticipation in inflammation. J Clin Invest 2003;111:25–27. [PubMed: 12511583]

Damiano BP, Cheung WM, Santulli RJ, Fung-Leung WP, Ngo K, Ye RD, Darrow AL, Derian CK, de Garavilla L, Andrade-Gordon P. Cardiovascular responses mediated by protease-activated receptor-2 (PAR- 2) and thrombin receptor (PAR-1) are distinguished in mice deficient in PAR-2 or PAR-1. J Pharmacol Exp Ther 1999;288:671–678. [PubMed: 9918574]

Farady CJ, Egea PF, Schneider EL, Darragh MR, Craik CS. Structure of an Fab-protease complex reveals a highly specific non-canonical mechanism of inhibition. J Mol Biol 2008;380:351–360. [PubMed: 18514224]

Fleming A, Copp AJ. Embryonic folate metabolism and mouse neural tube defects. Science 1998;280:2107–2109. [PubMed: 9641914]

Geelen JA, Langman J. Ultrastructural observations on closure of the neural tube in the mouse. Anat Embryol (Berl) 1979;156:73–88. [PubMed: 453553]

Godiksen S, Selzer-Plon J, Pedersen ED, Abell K, Rasmussen HB, Szabo R, Bugge TH, Vogel LK. Hepatocyte growth factor activator inhibitor-1 has a complex subcellular itinerary. Biochem J 2008;413:251–259. [PubMed: 18402552]

Greene ND, Copp AJ. Development of the vertebrate central nervous system: formation of the neural tube. Prenat Diagn 2009;29:303–311. [PubMed: 19206138]

Griffin CT, Srinivasan Y, Zheng YW, Huang W, Coughlin SR. A role for thrombin receptor signaling in endothelial cells during embryonic development. Science 2001;293:1666–1670. [PubMed: 11533492]

Guo H, Liu D, Gelbard H, Cheng T, Insalaco R, Fernandez JA, Griffin JH, Zlokovic BV. Activated protein C prevents neuronal apoptosis via protease activated receptors 1 and 3. Neuron 2004;41:563–572. [PubMed: 14980205]

Gustavsson P, Greene ND, Lad D, Pauws E, de Castro SC, Stanier P, Copp AJ. Increased expression of Grainyhead-like-3 rescues spina bifida in a folate-resistant mouse model. Hum Mol Genet 2007;16:2640–2646. [PubMed: 17720888]

Hansson L, Backman A, Ny A, Edlund M, Ekholm E, Ekstrand Hammarstrom B, Tornell J, Wallbrandt P, Wennbo H, Egelrud T. Epidermal overexpression of stratum corneum chymotryptic enzyme in mice: a model for chronic itchy dermatitis. J Invest Dermatol 2002;118:444–449. [PubMed: 11874483]

Harden N, Loh HY, Chia W, Lim L. A dominant inhibitory version of the small GTP-binding protein Rac disrupts cytoskeletal structures and inhibits developmental cell shape changes in Drosophila. Development 1995;121:903–914. [PubMed: 7720592]

Henrique D, Adam J, Myat A, Chitnis A, Lewis J, Ish-Horowicz D. Expression of a Delta homologue in prospective neurons in the chick. Nature 1995;375:787–790. [PubMed: 7596411]

Kahn ML, Nakanishi-Matsui M, Shapiro MJ, Ishihara H, Coughlin SR. Protease-activated receptors 1 and 4 mediate activation of human platelets by thrombin. J Clin Invest 1999;103:879–887. [PubMed: 10079109]

Kirchhofer D, Peek M, Li W, Stamos J, Eigenbrot C, Kadkhodayan S, Elliott JM, Corpuz RT, Lazarus RA, Moran P. Tissue expression, protease specificity, and Kunitz domain functions of hepatocyte growth factor activator inhibitor-1B (HAI-1B), a new splice variant of HAI-1. J Biol Chem 2003;278:36341–36349. [PubMed: 12815039]

Klezovitch O, Chevillet J, Mirosevich J, Roberts RL, Matusik RJ, Vasioukhin V. Hepsin promotes prostate cancer progression and metastasis. Cancer Cell 2004;6:185–195. [PubMed: 15324701]

Leyvraz C, Charles RP, Rubera I, Guitard M, Rotman S, Breiden B, Sandhoff K, Hummler E. The epidermal barrier function is dependent on the serine protease CAP1/Prss8. J Cell Biol 2005;170:487–496. [PubMed: 16061697]

List K, Bugge TH, Szabo R. Matriptase: potent proteolysis on the cell surface. Mol Med 2006;12:1–7. [PubMed: 16838070]

List K, Haudenschild CC, Szabo R, Chen W, Wahl SM, Swaim W, Engelholm LH, Behrendt N, Bugge TH. Matriptase/MT-SP1 is required for postnatal survival, epidermal barrier function, hair follicle development, and thymic homeostasis. Oncogene 2002;21:3765–3779. [PubMed: 12032844]

List K, Hobson JP, Molinolo A, Bugge TH. Co-localization of the channel activating protease prostasin/(CAP1/PRSS8) with its candidate activator, matriptase. J Cell Physiol 2007;213:237–245. [PubMed: 17471493]

List K, Kosa P, Szabo R, Bey AL, Wang CB, Molinolo A, Bugge TH. Epithelial integrity is maintained by a matriptase-dependent proteolytic pathway. Am J Pathol 2009;175:1453–1463. [PubMed: 19717635]

List K, Szabo R, Molinolo A, Sriuranpong V, Redeye V, Murdock T, Burke B, Nielsen BS, Gutkind JS, Bugge TH. Deregulated matriptase causes ras-independent multistage carcinogenesis and promotes ras-mediated malignant transformation. Genes Dev 2005;19:1934–1950. [PubMed: 16103220]

Ludeman MJ, Zheng YW, Ishii K, Coughlin SR. Regulated shedding of PAR1 N-terminal exodomain from endothelial cells. J Biol Chem 2004;279:18592–18599. Epub 12004 Feb 18524. [PubMed: 14982936]

Mackman N. Role of tissue factor in hemostasis, thrombosis, and vascular development. Arterioscler Thromb Vasc Biol 2004;24:1015–1022. [PubMed: 15117736]

Massa V, Greene ND, Copp AJ. Do cells become homeless during neural tube closure? Cell Cycle 2009;8:2479–2480. [PubMed: 19657232]

Nakanishi-Matsui M, Zheng YW, Sulciner DJ, Weiss EJ, Ludeman MJ, Coughlin SR. PAR3 is a cofactor for PAR4 activation by thrombin. Nature 2000;404:609–613. [PubMed: 10766244]

Netzel-Arnett S, Currie BM, Szabo R, Lin CY, Chen LM, Chai KX, Antalis TM, Bugge TH, List K. Evidence for a matriptase-prostasin proteolytic cascade regulating terminal epidermal differentiation. J Biol Chem 2006;281:32941–32945. [PubMed: 16980306]

Oberst MD, Williams CA, Dickson RB, Johnson MD, Lin CY. The activation of matriptase requires its noncatalytic domains, serine protease domain, and its cognate inhibitor. J Biol Chem 2003;278:26773–26779. [PubMed: 12738778]

Offermanns S, Zhao LP, Gohla A, Sarosi I, Simon MI, Wilkie TM. Embryonic cardiomyocyte hypoplasia and craniofacial defects in G alpha q/G alpha 11-mutant mice. EMBO J 1998;17:4304–4312. [PubMed: 9687499]

Oikonomopoulou K, Hansen KK, Saifeddine M, Vergnolle N, Tea I, Blaber M, Blaber SI, Scarisbrick I, Diamandis EP, Hollenberg MD. Kallikrein-mediated cell signalling: targeting proteinase-activated receptors (PARs). Biol Chem 2006;387:817–824. [PubMed: 16800746]

Regard JB, Kataoka H, Cano DA, Camerer E, Yin L, Zheng YW, Scanlan TS, Hebrok M, Coughlin SR. Probing cell type-specific functions of Gi in vivo identifies GPCR regulators of insulin secretion. J Clin Invest 2007;117:4034–4043. [PubMed: 17992256]

Riewald M, Ruf W. Mechanistic coupling of protease signaling and initiation of coagulation by tissue factor. Proc Natl Acad Sci U S A 2001;98:7742–7747. [PubMed: 11438726]

Ruppel KM, Willison D, Kataoka H, Wang A, Zheng YW, Cornelissen I, Yin L, Xu SM, Coughlin SR. Essential role for Galpha13 in endothelial cells during embryonic development. Proc Natl Acad Sci U S A 2005;102:8281–8286. [PubMed: 15919816]

Sambrano GR, Weiss EJ, Zheng YW, Huang W, Coughlin SR. Role of thrombin signalling in platelets in haemostasis and thrombosis. Nature 2001;413:74–78. [PubMed: 11544528]

Schoenwolf GC, Smith JL. Mechanisms of neurulation: traditional viewpoint and recent advances. Development 1990;109:243–270. [PubMed: 2205465]

Soifer SJ, Peters KG, O'Keefe J, Coughlin SR. Disparate temporal expression of the prothrombin and thrombin receptor genes during mouse development. Am J Pathol 1994;144:60–69. [PubMed: 8291612]

Sugihara K, Nakatsuji N, Nakamura K, Nakao K, Hashimoto R, Otani H, Sakagami H, Kondo H, Nozawa S, Aiba A, et al. Rac1 is required for the formation of three germ layers during gastrulation. Oncogene 1998;17:3427–3433. [PubMed: 10030666]

Sun J, Pons J, Craik CS. Potent and selective inhibition of membrane-type serine protease 1 by human single-chain antibodies. Biochemistry 2003;42:892–900. [PubMed: 12549907]

Szabo R, Hobson JP, Christoph K, Kosa P, List K, Bugge TH. Regulation of cell surface protease matriptase by HAI2 is essential for placental development, neural tube closure and embryonic survival in mice. Development 2009;136:2653–2663. [PubMed: 19592578]

Szabo R, Hobson JP, List K, Molinolo A, Lin CY, Bugge TH. Potent inhibition and global co-localization implicate the transmembrane Kunitz-type serine protease inhibitor hepatocyte growth factor activator inhibitor-2 in the regulation of epithelial matriptase activity. J Biol Chem 2008;283:29495–29504. [PubMed: 18713750]

Takeuchi T, Harris JL, Huang W, Yan KW, Coughlin SR, Craik CS. Cellular localization of membrane-type serine protease 1 and identification of protease-activated receptor-2 and single-chain urokinase-type plasminogen activator as substrates. J Biol Chem 2000;275:26333–26342. [PubMed: 10831593]

Takeuchi T, Shuman MA, Craik CS. Reverse biochemistry: use of macromolecular protease inhibitors to dissect complex biological processes and identify a membrane-type serine protease in epithelial cancer and normal tissue. Proc Natl Acad Sci U S A 1999;96:11054–11061. [PubMed: 10500122]

Ting SB, Wilanowski T, Auden A, Hall M, Voss AK, Thomas T, Parekh V, Cunningham JM, Jane SM. Inositol- and folate-resistant neural tube defects in mice lacking the epithelial-specific factor Grhl-3. Nat Med 2003;9:1513–1519. [PubMed: 14608380]

Vergnolle N. Review article: proteinase-activated receptors - novel signals for gastrointestinal pathophysiology. Aliment Pharmacol Ther 2000;14:257–266. [PubMed: 10735917]

Vergnolle N, Wallace JL, Bunnett NW, Hollenberg MD. Protease-activated receptors in inflammation, neuronal signaling and pain. Trends Pharmacol Sci 2001;22:146–152. [PubMed: 11239578]

Vouret-Craviari V, Grall D, Van Obberghen-Schilling E. Modulation of Rho GTPase activity in endothelial cells by selective proteinase-activated receptor (PAR) agonists. J Thromb Haemost 2003;1:1103–1111. [PubMed: 12871383]

Vu TK, Hung DT, Wheaton VI, Coughlin SR. Molecular cloning of a functional thrombin receptor reveals a novel proteolytic mechanism of receptor activation. Cell 1991;64:1057–1068. [PubMed: 1672265]

Wang JK, Lee MS, Tseng IC, Chou FP, Chen YW, Fulton A, Lee HS, Chen CJ, Johnson MD, Lin CY. Polarized epithelial cells secrete matriptase as a consequence of zymogen activation and HAI-1-mediated inhibition. Am J Physiol Cell Physiol 2009;297:C459–470. [PubMed: 19535514]

Waterman RE. Topographical changes along the neural fold associated with neurulation in the hamster and mouse. Am J Anat 1976;146:151–171. [PubMed: 941847]

Wilson S, Greer B, Hooper J, Zijlstra A, Walker B, Quigley J, Hawthorne S. The membrane-anchored serine protease, TMPRSS2, activates PAR-2 in prostate cancer cells. Biochem J 2005;388:967–972. [PubMed: 15537383]

Zohn IE, Sarkar AA. Modeling neural tube defects in the mouse. Curr Top Dev Biol 2008;84:1–35. [PubMed: 19186242]

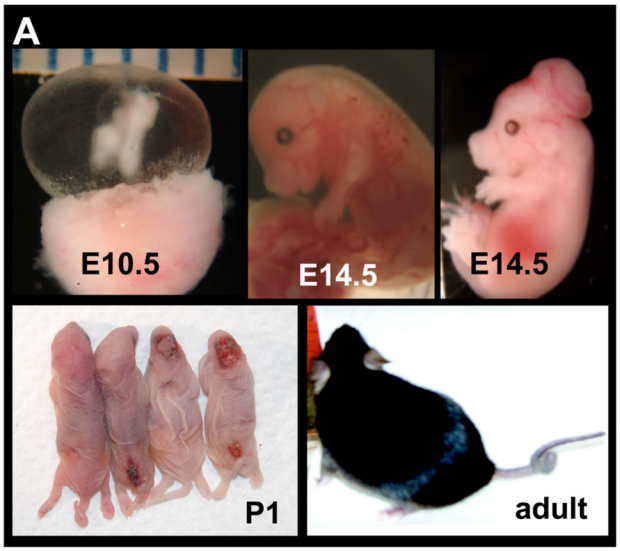

B

Day PC	*Par1+/-:Par2+/-* x *Par1+/-:Par2+/-* +/+:+/+	+/-:+/-	-/-:-/- (Ex)
12.5	27	63	9 (3)
14.5	7	8	2 (2)

	Par1-/-:Par2-/- x *Par1+/-:Par2+/-* +/-:+/-	-/-:-/- (Ex)
9.5	49	44
10.5	38	17
11.5-12.5	40	12 (4)
13.5-14.5	31	9 (3)
15.5-16.5	39	6 (1)
17.5-19.5	30	13 (4)

C

Tie2p/e-Par1$^{0/0}$ *Par1Par2* genotype (# exencephalic)			*Tie2p/e-Par1*$^{+/0}$ *Par1Par2* genotype (# exencephalic)		
+/+:+/+	+/-:+/-	-/-:-/-	+/+:+/+	+/-:+/-	-/-:-/-
48	71	9 (1)	29	75	25 (5)

D

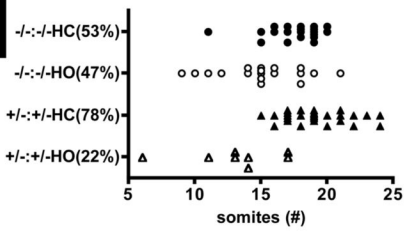

E

	hindbrain open	hindbrain closed
Par1+/-:Par2+/-	1	26
Par1-/-:Par2-/-	9	19

Figure 1. Phenotypes associated with combined deficiency of Par2 and Par1

(A) Three phenotypes exhibited by *Par1*$^{-/-}$*:Par2*$^{-/-}$ embryos: mid-gestational cardiovascular failure (top left); late-gestational death associated with edema (top center) and exencephaly (top right). *Par1*$^{-/-}$*:Par2*$^{-/-}$ embryos that survived to birth showed exencephaly and spina bifida with incomplete penetrance (lower left; from left to right: curly tail, spina bifida/curly tail, anencephaly, anencephaly and spina bifida/curly tail). A surviving adult with curly tail is at lower right. (B,C) Viability and presence of exencephaly at various gestational ages (B) and in the presence or absence of an endothelial Par1 transgene (C); # alive (# with exencephaly) is shown. Embryos in (C) were collected at 12.5–14.5 dpc. (D, E) Embryos from *Par1*$^{+/-}$*:Par2*$^{+/-}$ *X Par1*$^{-/-}$*:Par2*$^{-/-}$ crosses were collected at 9.5 dpc, scored for an open HO or closed HC hindbrain neuropore and somite count, then genotyped. To visualize the neuropore, embryos were X-gal stained. (E) Results from embryos in (D) with 15 or more somites. See also Figure S1.

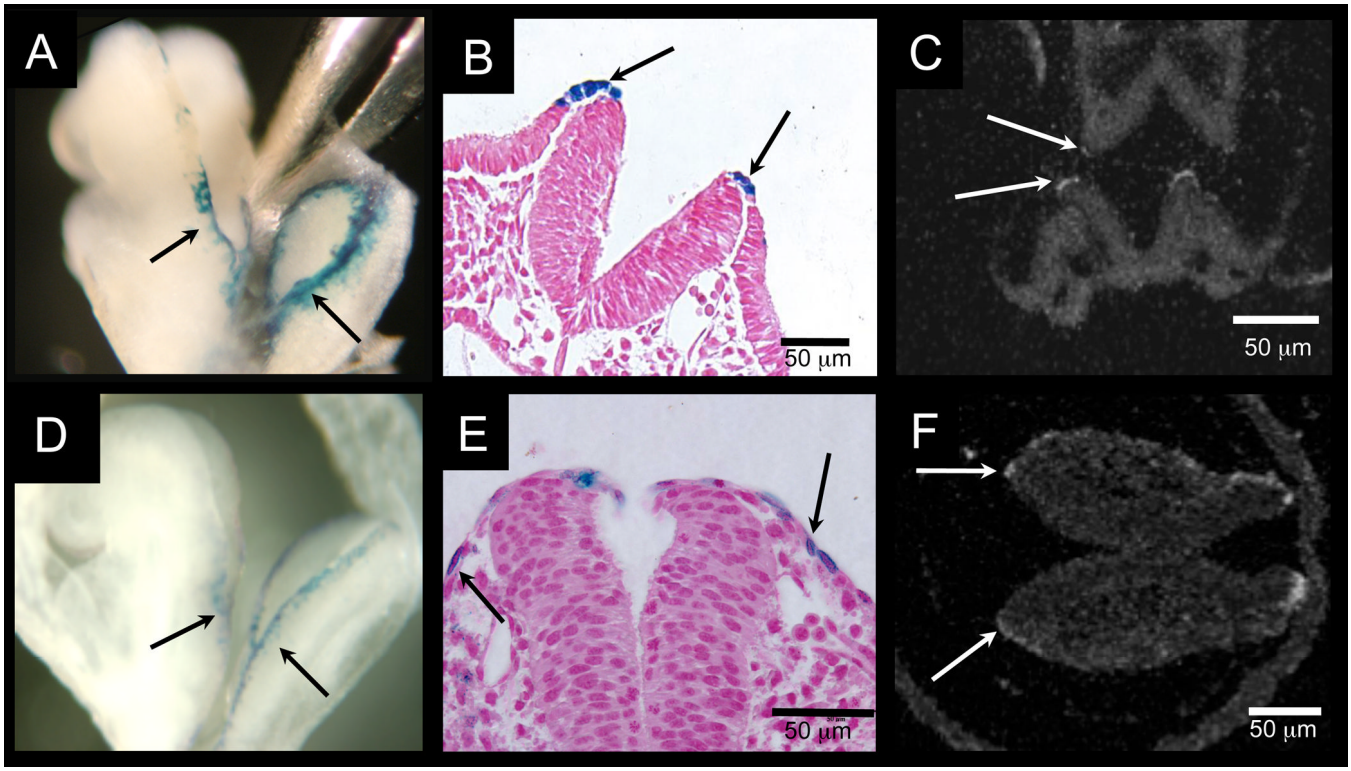

Figure 2. Localized expression of *Par2* in surface ectoderm and characterization of a surface ectoderm Cre (*Grhl3*^{Cre})

(A–C) Par2 expression at the time of neural tube closure. (A,B) X-gal staining of Par2-lacZ knock-in embryo in whole mount (A) and cross section (B). In situ hybridization of wild-type embryos for *Par2* mRNA (C). (D, E) LacZ expression from a Cre-IRES-NLSlacZ cassette inserted into the *Grhl3* locus (Grhl3^{Cre}; see Figure S3). (F) In situ hybridization of wild-type embryo for *Grhl3* mRNA. Sense controls for C and F are in Figure S2. Embryos were collected at about 9.25 dpc.

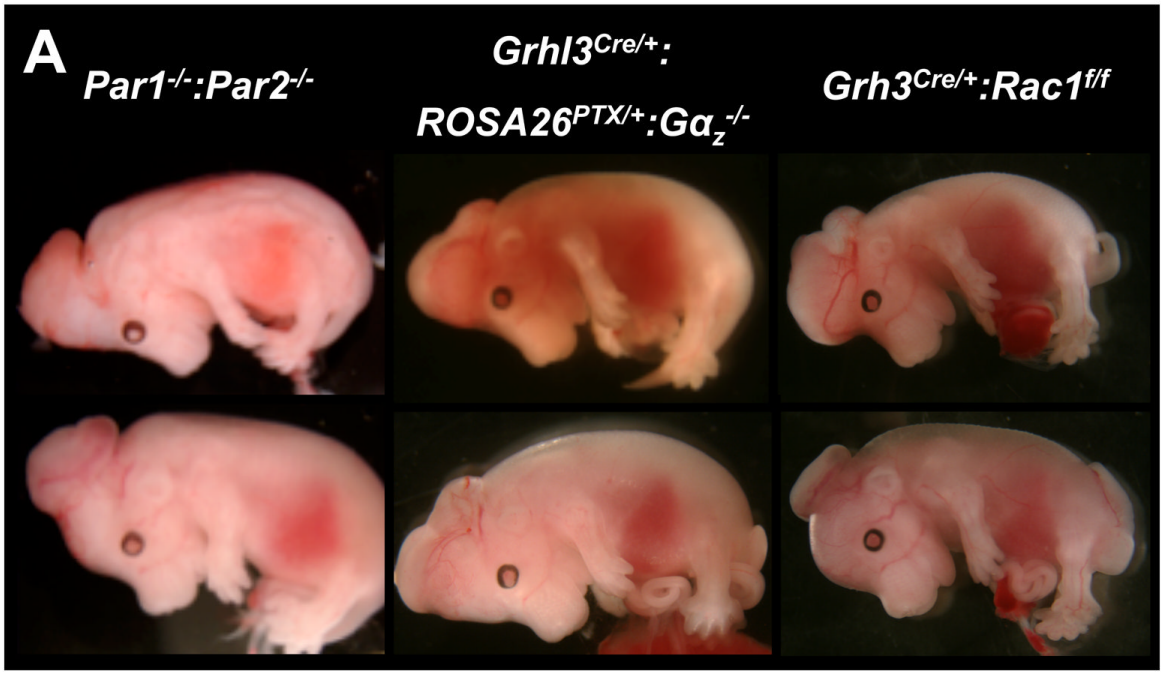

B

	Grhl3$^{+/+}$		*Grhl3*$^{Cre/+}$	
	exenceph (%)	posterior NTD (%)	exenceph (%)	posterior NTD (%)
ROSA26$^{PTX/}$:*Gα*$_z^{+/+}$	0/15 (0)	0/15 (0)	2/21 (10)	0/21 (0)
ROSA26$^{PTX/}$:*Gα*$_z^{+/-}$	0/24 (0)	0/24 (0)	1/27 (4)	5/27 (18)
ROSA26$^{PTX/}$:*Gα*$_z^{-/-}$	0/10 (0)	0/10 (0)	3/15 (20)	6/15 (40)
Rac1$^{f/+}$	0/11 (0)	0/11 (0)	0/15 (0)	0/15 (0)
Rac1$^{f/f}$	0/7 (0)	0/7 (0)	7/12 (58)	10/12 (83)
Rac1$^{f/+}$ (folate)	0/15 (0)	0/15 (0)	0/14 (0)	0/14 (0)
Rac1$^{f/f}$ (folate)	1/12 (8)	0/12 (0)	8/13 (62)	10/13 (77)

Figure 3. Abrogating G_i function and Rac1 expression in surface ectoderm causes neural tube defects

(A) Exencephaly in *Par1*$^{-/-}$:*Par2*$^{-/-}$, *Grhl3*$^{Cre/+}$:*ROSA26*$^{PTX/+}$:G$\alpha_z^{-/-}$, and *Grhl3*$^{Cre/+}$:*Rac1*$^{f/f}$ embryos collected at 14.5 dpc. Spina bifida and curly tail in *Grhl3*$^{Cre/+}$:*ROSA26*$^{PTX/+}$: G$\alpha_z^{-/-}$ (lower) and *Grhl3*$^{Cre/+}$:*Rac1*$^{f/f}$ (both) embryos. (B) Occurrence of neural tube defects (# with NTD/# live (%)) by genotype at 14.5 dpc. See also Figure S3.

A

protease	Gene symbol	ΔCT abundance relative to control (n=4)	$2^{\Delta\Delta CT}$ abundance relative to Par2 (n=4)	$2^{\Delta\Delta CT}$ enrichment in surface ectoderm (n=2)
klk8	Klk8	7.3 +/- 0.4	25 +/- 10	1.0 +/- 0.1
prostasin	Prss8	7.7 +/- 1.3	23 +/- 5.9	**3.2 +/- 0.9**
tPA	Plat	8.7 +/- 0.4	8.9 +/- 6.5	1.0 +/- 0.1
epitheliasin	Tmprss2	9.1 +/- 1.7	9.6 +/- 6.2	**1.5 +/- 0.2**
masp1	Masp1	9.2 +/- 0.3	4.8 +/- 2.8	1.2 +/- 0.2
polyserase-2	Prss36	9.5 +/- 0.3	5.3 +/- 2.6	1.0 +/- 0.0
matriptase	St14	9.5 +/- 0.5	5.2 +/- 1.9	**2.5 +/- 0.2**
hepsin	Hpn	9.6 +/- 1.3	6.6 +/- 3.0	**2.2 +/- 0.3**
cfb	Cfb	10 +/- 0.6	3.3 +/- 1.5	1.1 +/- 0.2
chymopasin	Ctrl	11 +/- 0.5	1.8 +/- 1.3	Undetectable
Par1	F2r	5.5 +/- 0.4	76 +/- 52	1.0
Par2	F2rl1	12 +/-1		5.8

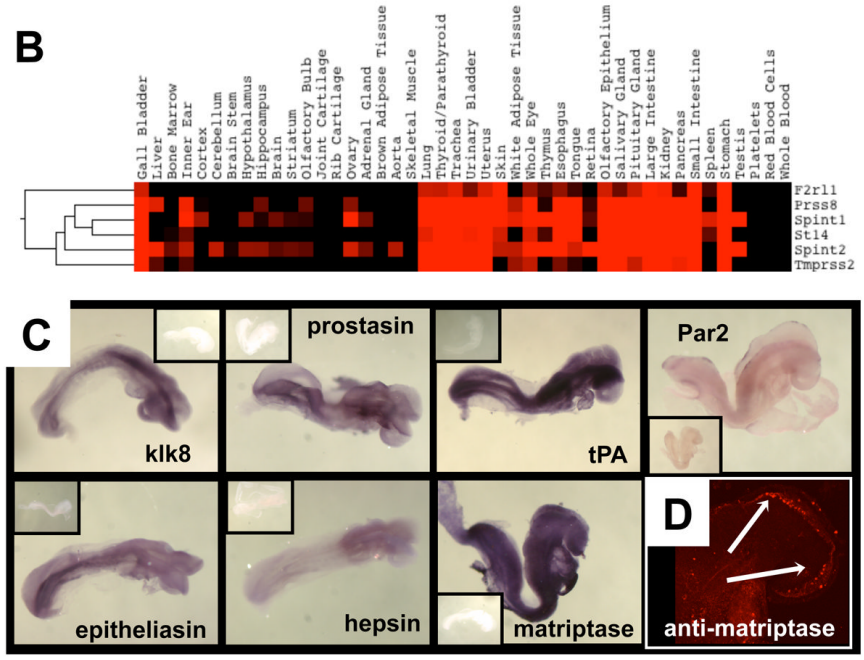

Figure 4. Identification of candidate Par2 activators expressed during neural tube closure

(A) Expression of 125 serine proteases predicted to reside in the extracellular space by real-time PCR of RNA from pooled wild-type embryos collected at 8.5–9.5 dpc. The ten most abundantly expressed relative to housekeeping genes (ΔCT), their abundance relative to Par2 ($2^{\Delta\Delta CT}$) and their enrichment in surface ectoderm (expression in YFP-positive surface ectoderm cells sorted from dissociated $Grhl3^{Cre+/-}$:$ROSA26^{YFP/+}$ (ROSA26 Lox-STOP-Lox YFP) embryos relative to YFP-negative cells from the same embryos ($2^{\Delta\Delta CT}$)) are shown. (B) Hierarchical cluster analysis was used to compare expression patterns of 125 candidate proteases, 11 select inhibitors and Par2 was measured by real-time PCR of RNA from 44 tissues and circulating cells from adult mice. The cluster containing Par2, matriptase (St14), prostasin

(prss8) and their inhibitors Hai-1 (Spint1) and Hai-2 (Spint2) is shown in TreeView; red intensity indicates increased expression. See Document S3 for entire cluster analysis and S1 for experimental procedures. (C) Surface ectoderm expression of mRNA for the indicated candidate proteases and Par2 by whole-mount in situ hybridization of 8.5 dpc embryos; sense controls are in insets. (D) Immunostaining of live 8.5 dpc embryos with E2, an antibody specific for the active form of matriptase. Arrows indicate staining of surface ectoderm overlying the hindbrain neuropore. Close-up is in Figure S4.

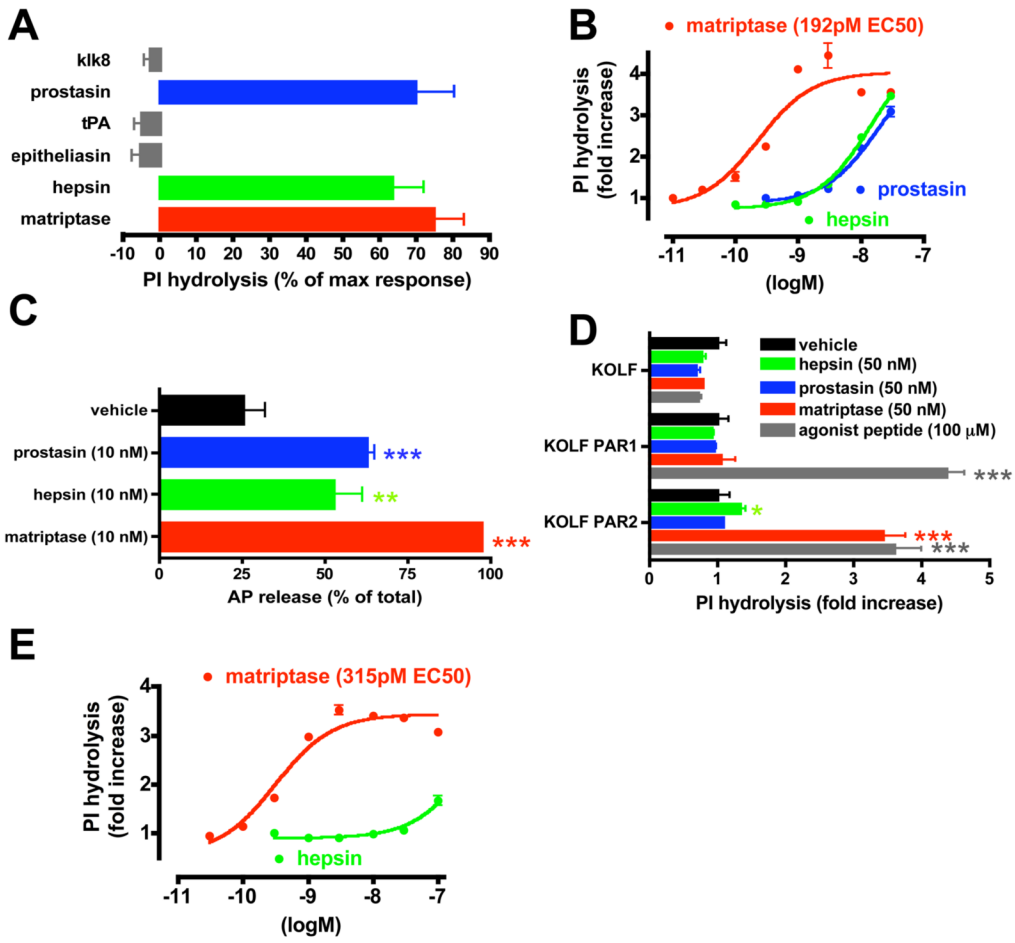

Figure 5. Par2 cleavage and activation by membrane-associated proteases

(A,B,E) Protease-triggered phosphoinositide (PI) hydrolysis in response to candidate Par2-activating proteases. (A) PI hydrolysis in HaCaT cultures after addition of soluble recombinant protease domains (50 nM) expressed as % of the response to maximal concentrations of PAR-activating peptides (100 μM TFLLRN + 100 μM SLIGRL). (B) Concentration response to protease domains that showed activity in (A). (C) Alkaline phosphatase (AP) release upon addition of soluble protease domains to HaCaTs transiently expressing an N-terminal AP–Par2 fusion protein. See Figure S5 for cleavage site specificity and PAR selectivity. (D) PI hydrolysis triggered by recombinant soluble protease domains or a maximal concentration (100 μM) of PAR1 or PAR2 peptide agonist (or both peptides for untransfected KOLFs) in KOLFs stably transfected with PAR1 or PAR2. Similar results were obtained in three separate experiments. (E) PI hydrolysis in PAR2-expressing KOLFs, concentration response to matriptase and hepsin.

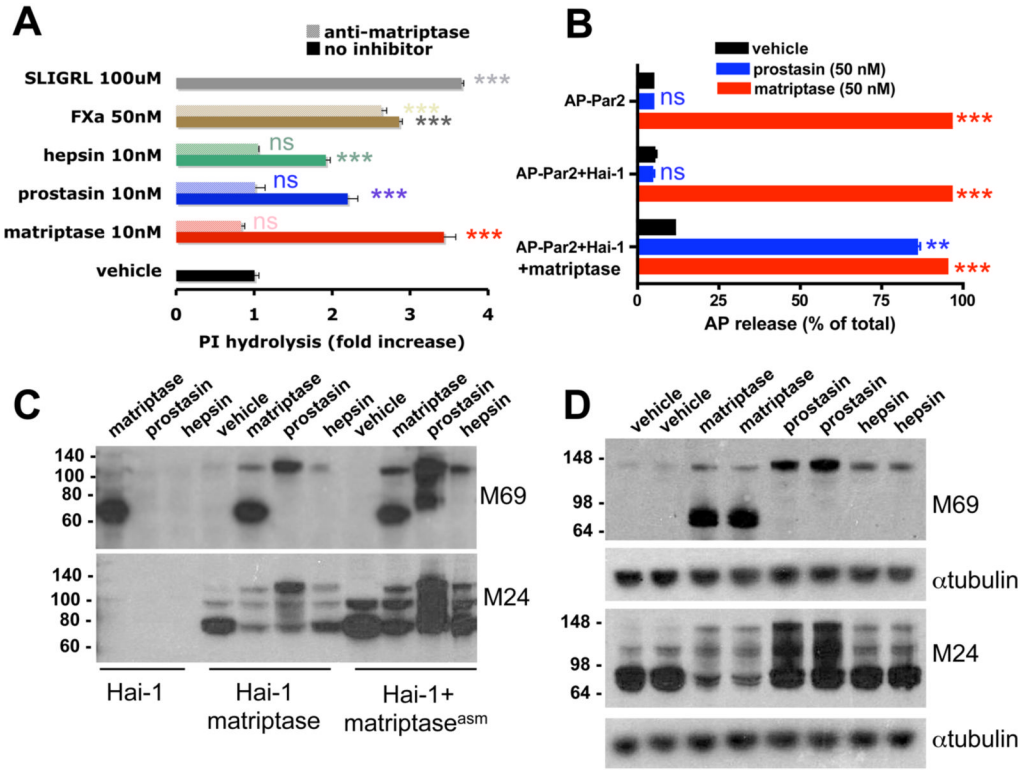

Figure 6. Evidence for a cascade from prostasin and hepsin to matriptase to Par2 activation

(A) Inhibition of protease-triggered PI hydrolysis in HaCaT by E2 (2 μM), an active site-blocking antibody to matriptase. (B) Par2 cleavage by prostasin in KOLFs transiently transfected with expression vectors for mouse AP-Par2, Hai-1 and full-length matriptase as indicated. AP release in response to addition of soluble recombinant prostasin or matriptase (50nM) was measured. (C) Immunoblot analysis of matriptase processing by prostasin and hepsin in KOLFs transfected with Hai-1 alone or Hai-1 plus matriptase or matriptase active site mutant (asm) expression vectors. Cultures were treated with the soluble recombinant protease domains (50 nM) indicated at top; lysates were immunoblotted with M69 and M24 matriptase antibodies, which recognize the active processed form and total matriptase, respectively. (D) Conversion of endogenously expressed matriptase zymogen to its active form by prostasin and hepsin in HaCaT cultures. Cultures were treated with the indicated soluble recombinant protease domains and cell lysates analyzed as in (C). Tubulin blot served as a loading control. See also Figure S6.